Dentomaxillofacial Radiology (2023) 52, 20230030

birpublications.org/dmfr

RESEARCH ARTICLE

The efficacy of supervised learning and semi-supervised learning in diagnosis of impacted third molar on panoramic radiographs through artificial intelligence model

[1]Ji-Youn Kim, [2]Se Hoon Kahm, [3]Seok Yoo, [4]Soo-Mi Bae, [5]Ji-Eun Kang and [2]Sang Hwa Lee

[1]Division of Oral & Maxillofacial Surgery, Department of Dentistry, St. Vincent's Hospital, College of Medicine, The Catholic University of Korea, Seoul, Republic of Korea; [2]Department of Dentistry, Eunpyeong St. Mary's Hospital, College of Medicine, The Catholic University of Korea, Seoul, Republic of Korea; [3]AI Business Headquarters, Unidocs Inc., Seoul, South Korea; [4]Department of Artificial Intelligence, Graduate school, Korea University, Seoul, South Korea; [5]JINHAKapply Corp., Seoul, South Korea

Objectives: The aim of the study was to evaluate the efficacy of traditional supervised learning (SL) and semi-supervised learning (SSL) in the classification of mandibular third molars (Mn3s) on panoramic images. The simplicity of preprocessing step and the outcome of the performance of SL and SSL were analyzed.
Methods: Total 1625 Mn3s cropped images from 1000 panoramic images were labeled for classifications of the depth of impaction (D class), spatial relation with adjacent second molar (S class), and relationship with inferior alveolar nerve canal (N class). For the SL model, WideResNet (WRN) was applicated and for the SSL model, LaplaceNet (LN) was utilized.
Results: In the WRN model, 300 labeled images for D and S classes, and 360 labeled images for N class were used for training and validation. In the LN model, only 40 labeled images for D, S, and N classes were used for learning. The F1 score were 0.87, 0.87, and 0.83 in WRN model, 0.84, 0.94, and 0.80 for D class, S class, and N class in the LN model, respectively.
Conclusions: These results confirmed that the LN model applied as SSL, even utilizing a small number of labeled images, demonstrated the satisfactory of the prediction accuracy similar to that of the WRN model as SL.
Dentomaxillofacial Radiology (2023) **52**, 20230030. doi: 10.1259/dmfr.20230030

Cite this article as: Kim J-Y, Kahm SH, Yoo S, Bae S-M, Kang J-E, Lee SH. The efficacy of supervised learning and semi-supervised learning in diagnosis of impacted third molar on panoramic radiographs through artificial intelligence model. *Dentomaxillofac Radiol* (2023) 10.1259/dmfr.20230030.

Keywords: deep learning; third molar; panoramic radiography; supervised machine learning; semi-supervised learning

Introduction

Panoramic radiography is the first-choice diagnostic tool to evaluate the third molar extraction difficulty. The surgical difficulty and complication risk could be evaluated through the information about the depth of impaction, and spatial relation to adjacent anatomic structures such as a second molar, inferior alveolar nerve canal, and maxillary sinus obtained from this 2D image. Based on the panoramicradiography findings, the decision to take additional cone beam computed tomography (CBCT) images and/or referral to an oral and maxillofacial surgeon can be performed. According to the surgical difficulty, the operation planning including time schedule and instrument tool preparation is organized. Also, it serves as the medical insurance claim data recording.[1,2]

Correspondence to: Professor Sang Hwa Lee, E-mail: justina@catholic.ac.kr

Received 10 January 2023; revised 27 March 2023; accepted 18 April 2023; published online 16 May 2023

Recently studies about the application of artificial intelligent models in the analysis of medical[3–5] and dental images[6–9] were published.Most of the papers were based on the supervised deep-learning models (SL) that need large amounts of labeled training data. In real-world scenarios, we often find that labels are scarce, prone to error, time-consuming to collect, and require effort by specialized personnel for the labeled data. Therefore, obtaining a well-representative dataset is a major limitation of this machine learning model.

This limitation motivated the development of models that provide less reliance on the labeled data model and reduced complexity such as semi-supervised deep learning (SSL). The purpose of SSL is to extract information from unlabeled data in combination with a small amount of labeled data while producing results comparable to traditional SL.[10,11] Recent SSL studies have shown remarkably accurate results comparable to SL studies. And the gap between both models is much smaller now than it was even a few years ago.[12–15] However, the application of SSL model on dental panoramic image analysis is not well studied.

In this study, the efficacy of traditional SL and SSL in the classification of mandibular third molars (Mn3s) on the panoramic images were evaluated to access the simplicity of preprocessing step and the outcome of the performance.

Methods and materials

Ethical approval

This study was conducted in accordance with the guidelines of the World Medical Association Helsinki Declaration for biomedical research involving human subjects. This study was approved by the Institutional Review Board (IRB) and Clinical Data Warehouse (CDW) data review board of the Catholic University of Korea, Catholic Medical Center(CIRB-20210503–001). The IRB waived the written documentation of informed consent. Data were collected and administrated by CDW and the images were exported under supervise of Enterprise Data Platform (EDP) of The Catholic University of Korea Catholic Information Convergence Institute.

Table 1 Three categories of classifications of mandibular third molars

Class	Subclass	Definition of classification
Depth of impaction (D)	D0	Mn3 was missed
	D1	Entire crown was uncovered by the bone,
	D2	Less of 2/3 crown part was covered by the bone
	D3	The 2/3 or more of crown part was covered by the bone
Spatial relation (S)	S0	Mn3 was missed
	S1	Close to parallel
	S2	Close to Mesio-angulation
	S3	Close to perpendicular
Relationship with IAN (N)	N1	No contact with IAN
	N2	Contact with IAN

IAN, inferior alveolar nerve canal; Mn3, mandibular third molar.

Data collection

We searched retrospectively the list of subjects who visited Eunpyeong St. Mary's Hospital, St. Vincent Hospital, or Seoul St. Mary's Hospital of Catholic Medical Center from 2016 to 2020 with panoramic image taken under a diagnosis of "impacted tooth". Panoramic radiographs were obtained using ProMax (Planmeca, Helsingki, Finland) or Kodak 8000 Digital Panoramic System (Carestream Health Inc., NY, USA) according to the user manual. The patient's data list was subjected to an automatic de-identification under the CDW system. From the collected list, approximately 16,475 panoramic images were downloaded and protected by the EDP system in JPEG format. Of these radiographs, 1000 images were randomly selected and labeled. From a total of 1000 panoramic images, 1625 Mn3s cropped images were prepared for learning. The panorama radiographs with low resolution or pathologic lesion such as cyst and tumors were excluded (Figure 1).

Data preprocessing for classification

Each third molar was classified based on the depth of impaction, the spatial relation to adjacent second molars, and the relationship with inferior alveolar nerve canal of Mn3 (Table 1):

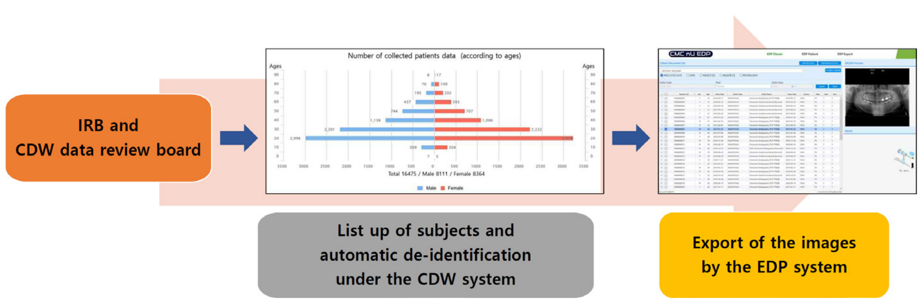

Figure 1 Summary of data collection process IRB, Institutional Review Board; CDW, Clinical Data Warehouse; EDP, Enterprise Data Platform

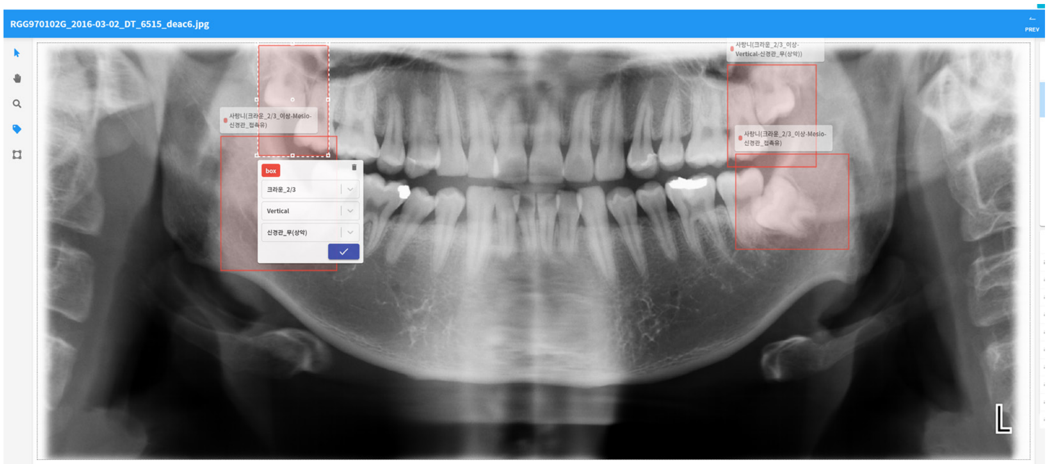

Figure 2 Labeled classification of mandibular third molars through web-based data labeling tool

1. D class: The impacted crown level of Mn3 into the alveolar bone was set as the evaluation point. When the Mn3 was missed, D class was recorded as D0. When its entire crown was uncovered by the bone, it was classified as D1. When less than 2/3 of the crown part was covered by the bone, it was recorded as D2. When 2/3 or more of the crown part was covered by the bone, we marked it as D3.

2. S class: The long axis of Mn3 was compared with the adjacent second molar. When the Mn3 was missed, the S class was recorded as S0. When they were close to parallel, it was recorded as S1 (vertical). When they were close to perpendicular, we marked it as S3 (horizontal). Otherwise, it was recorded as S2 (mesial) when the long axis of Mn3 was inclined to mesial. We excluded the disto-angulation subclass because it has a much smaller number of cases than the other S subclasses. This is because cases where Mn3s are distoangulated clinically are rare compared to other angles.

3. N class: When the Mn3 was not in contact with the inferior alveolar nerve canal, the N class was recorded as N1. When the Mn3 was in contact with the inferior alveolar nerve canal, we marked as N2.
Web-based data labeling tool was installed in The Catholic University of Korea Catholic Information Convergence Institute. Two oral and maxillofacial surgeons classified each category and marked a bounding box as Region of Interest (ROI) on Mn3s manually (Figure 2). Every labeled subclass was cross-verified. Images with complete agreement by both surgeons were used for learning. Every bounding box was cropped and resized to 264 × 264 pixels. Since the number of instances for each class was unbalanced, a rule has been established that at least one subclass must have at least 100 instances. The number of instances per subclass was made as uniform as possible within the collected dataset. Fewer subclasses were merged or excluded. Also, a re-sampling technique was applied to uniformly match the amount of data.

Modeling and learning

For WideResNet (WRN) model as the SL model, we used stochastic gradient descent as optimizer with a learning rate of 0.005, a mini-batch size of 8, and a momentum of 0.9. For LaplaceNet (LN) as the SSL model, the same optimizer with learning rate of 0.01, weight decay of 0.0005, mini-batch size of 40, and momentum of 0.9 was customized. Dataset for WRN was split into three disjoint sets, including a training set, a validation set, and a test set and the data set for LN was also split into three disjoint sets, including a labeled set, an unlabeled set, and a test set.In the WRN model, 300 labeled images for D and S classes, and 360 labeled images for N class were used as training and validation sets. In the LN model, only 40 labeled images for D, S, and N classes were used for learning. The number of images in the labeled set of LN was the same as that in the validation set of WRN; the number of images in the unlabeled set of LN was the same as in the training set of WRN; and the test set for LN had the same number of images for WRN (Table 2).

Performance analysis

The accuracy, sensitivity, precision, and f1 scores were calculated to evaluate the performance of each model. Python programming language (v. 3.7.11), Pytorch (v.1.8.2), and graphics card (Nvidia Quadro 6000 8 GB *2) were used for analysis.

Results

Table 3 shows the performances of WRN and LN model evaluated with accuracy, sensitivity, precision, and f1 scores. The best performance of WRN was obtained using 50 epochs.In the WRN model, the accuracy of D class, S class, and N class were 0.87, 0.91, and 0.86, respectively. The sensitivity of D class, S class, and N class were 0.88, 0.87, and 0.85, respectively. The precision of D class, S class, and N class were 0.90, 0.90, and

Table 2 Dataset for WideResNet and LaplaceNet

Model	Class	Subclass	Training set	Validation set	Test set
WideResNet	D	D0	65	10	19
		D1	65	10	12
		D2	65	10	79
		D3	65	10	72
		total	260	40	182
	S	S0	290	10	19
		S1	290	10	52
		S2	290	10	46
		S3	290	10	66
		total	1160	40	183
	N	N1	160	20	21
		N2	160	20	41
		total	320	40	62
Model	Class	Subclass	Labeled set	Unlabeled set	Test set
LaplaceNet	D	D0	10	65	19
		D1	10	65	12
		D2	10	65	79
		D3	10	65	72
		total	40	260	182
	S	S0	10	290	19
		S1	10	290	52
		S2	10	290	46
		S3	10	290	66
		total	40	1160	183
	N	N1	20	160	21
		N2	20	160	41
		total	40	620	62

D, depth of impaction of mandibular third molar; S, spatial relation with adjacent second molar of mandibular third molar; N, relationship with inferior alveolar nerve canal of mandibular third molar

0.85, respectively. The f1 scores of D class, S class, and N class were 0.87, 0.87, and 0.83, respectively. The best performance of the LN was obtained using 47 epochs in D class, 51 epochs in S class, and 160 epochs in N class. In the LN model, the accuracy of D class, S class, and N class were 0.80, 0.95, and 0.81, respectively. The sensitivity of D class, S class, and N class were 0.88, 0.95, and 0.85, respectively. The precision of D class, S class, and N class were 0.82, 0.94, and 0.82, respectively. The f1 scores of D class, S class, and N class were 0.84, 0.94, and 0.80, respectively. Figure 3 shows results of both WRN and LN models as a confusion matrix. Considering that the higher the diagonal value of the confusion matrix, the more accurately predictive model, the figure presented significant accurate diagnosis in both WRN and LN models.

Table 3 Results of classification performance through WideResNet and LaplaceNet

Model	*Class*	*Best epochs*	*Accuracy*	*Sensitivity*	*Precision*	*F1 score*
WideResNet	D	50	0.87	0.88	0.90	0.87
	S	50	0.91	0.87	0.90	0.87
	N	50	0.86	0.85	0.85	0.83
LaplaceNet	D	47	0.80	0.88	0.82	0.84
	S	51	0.95	0.95	0.94	0.94
	N	160	0.81	0.85	0.82	0.80

D, depth of impaction of mandibular third molar; S, spatial relation with adjacent second molar of mandibular third molar; N, relationship with inferior alveolar nerve canal of mandibular third molar

Discussion

In this study, classifications of the depth of impact, the spatial relation to the adjacent second molar, and the relationship with the inferior alveolar nerve canal of the Mn3s, which determine surgical difficulty and risk of nerve damage, were trained and predicted using two different deep learning models, a WRN as an SL model and an LN as an SSL model. Through this study, it was found that SSL with only 10 or 20 labeled images in each class that would require less time, effort, and cost in data preprocessing showed high accurate predictability (F1 score: 0.80–0.94), similar to that of the traditional SL model (F1 score: 0.83–0.87). To the best of our knowledge, this study is significant in that it is the first study using SSL for the classification of panoramic radiographs.

Surgical extraction of Mn3s is one of the most common surgical treatments performed by general dental practitioners and oral and maxillofacial surgeons worldwide.[1] Therefore, since the early days of deep learning applied to the dental field, the segmentation and classification of Mn3s and related IANs have been continuously studied.[7–9,16] In 2020, Fukuda et al.[7] reported the classification of the relationship between Mn3s and IANs in 600 labeled panoramic images using three different SL neural networks (AlexNet, GoogLeNet, and VGG-16). All three deep learning models showed good accuracies of 0.71–0.90.[7] In 2021, Yoo et al.[9] reported the classification of depth, ramal relationship, and angulation of Mn3s in 600 labeled panoramic images using ResNet-34. In their SL study, prediction accuracies for depth, ramal relationship, and spatial relationship (angulation) were 0.79, 0.82, and 0.90, respectively.[9] In our study, accuracies for the classification of the depth of impaction, spatial relation to adjacent second molar, and the relation between Mn3s and IANs were 0.87, 0.91, and 0.85, respectively, in the SL model using WRN. And 0.80, 0.95, and 0.81, respectively, in the SSL model with very few labeled images through LN in this study. It is very meaningful that the accuracy of SSL showed comparable results to the accuracy of SL in this study and previous studies.

WRN model as an SL model is a novel network with decreased depth and increased width of residual networks.[17] Because of that, the WRN provides better performance and faster training than previous deep

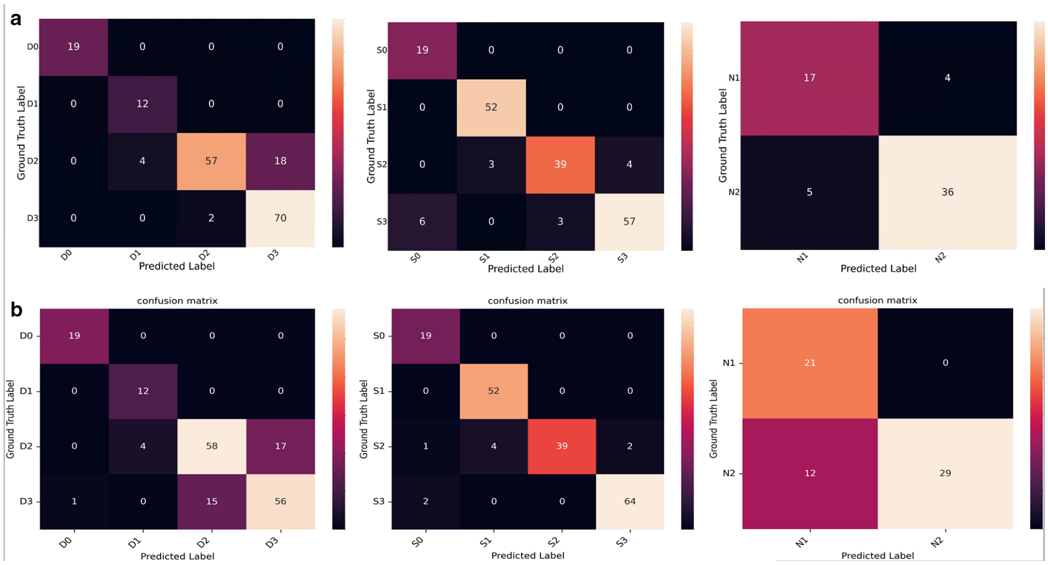

Figure 3 Confusion matrix of the classification results. A showed the result of WideResNet model. B showed the result of LaplaceNet model. D, depth of impaction of mandibular third molar; S, spatial relation with adjacent second molar of mandibular third molar; N, relationship with inferior alveolar nerve canal of mandibular third molar

learning networks, achieving new state-of-the-art (SOTA) and significant improvements on ImageNet.[17] Thus, deep learning using the WRN model has been actively studied in the analysis of medical images.[18–20] LN model as an SSL model is a graph-based pseudolabel approach for semi-supervised classification with greatly reduced model complexity and amount of labeled data required for deep learning.[10] LN model achieved SOTA for semi-supervised image classification in 2021.[10] However, so far, there has been no deep learning study using the LN model for the classification of medical-dental images to the best of our knowledge. Training deep learning models often rely on access to large amounts of labeled training data.[10] However, gathering a sufficient amount of labeled training medical data is unrealistic because it is impossible to share a large amounts of patients' private medical records between institutions. A single institution does not have many both normal and abnormal anatomical images in equal proportions (class imbalance).[14] To use images as training data, a complicated procedure according to medical ethics is required. In addition, it requires a lot of time and effort by several specialists who have expert medical knowledge in such a special medical field to collect a large amount of highly accurate labeled medical data. This process is too expensive and time-consuming. Thus, learning with less labeled data has been a longstanding challenge of artificial intelligence (AI) research.[12] At that point, the need for developing SSL with high accuracy comparable to SL is increasing, especially in the medical field.

In recent years, semi-supervised deep learning has been applied to the medical field. In 2021, Han et al[13] studied the SSL model adopting the architecture of efficient Net-b0 for discriminating between coronavirus disease 2019 (COVID-19) and common pneumonia CT images. In their study, the SSL model showed an accuracy of 97.32%, higher than the SL model used for comparison. In 2022, Kuo et al.[15] reported semi-supervised and automatic segmentation algorithm model by combining MobileNet, squeeze-and-excitation networks (SENet), and ResNet for scoring chronic rhinosinusitis from a total of 175 CT sets, with 50 participants. The SSL approach achieved SOTA performance for sinus segmentation and provided a sensitively reproducible scoring method for measuring the severity of chronic sinusitis compared to the traditional scoring system. In 2023, Qayyumetal.[21] reported dental caries detection and segmentation using the periapical radiographs. In this study, SSL using only 40 labeled images showed comparable accuracy with SL model. In our study, the SSL model with only 10 or 20 labeled images in each class adopting LN showed comparable accuracy, sensitivity, precision, and F1 score to the SL model adopting WRN. Especially, in the classification of spatial relation to adjacent second molar, the F1 score of the SSL approach (0.94) was higher than that of the SL approach (0.87). This might be because the number of instances for each class in the spatial classification showed an almost uniform distribution compared to the other two classifications. Various methods should be further considered to avoid the trivial collapse of representations problem of the SSL model that might occur due to class-specific instance imbalance that inevitably occurs in clinical medical images.[12]

This study also has some facts to consider. First of all, it is a known fact that to obtain reliable results, external validation using panoramic radiograph datasets from other institutions is necessary.[22] However, since each medical imaging data contain private personal information, such data are primarily protected and locked.and not easily accessible and shareable between different institutions due to medical ethical issues.[23] Nevertheless, this study is characterized by the collection and de-identification of the data from three different hospitals of our university using CDW system. And the panorama image files were downloaded and protected by the EDP system. We collected data from three hospitals located in different districts and different panorama equipment systems. It would be contributed to diminishing the overfitting

Second, for the SSL, we used the LN model that uses deep semi-supervised classification model learning.[10] So the bounding boxes we had marked in the panorama image were cropped and used for the classification, not for detection. Going one step further, in a future study, an SSL model with detection can automatically locate the teeth and analyzed them.

Conclusion

This perspective preliminary study was to focus on the SSL model that could be used for the classification of dental panoramic images, like SL model which has been studied in the field of deep learning. Thus, the study evaluated the efficacy of the SSL and SL models in the diagnosis of the impacted Mn3s on panorama image. LN model applied as SSL, even utilizing a small number of labeled images (only 10 or 20 labeled images in each class), demonstrated satisfactory results in accuracy, sensitivity, precision, and f1 scores. These outcomes were similar to that of the traditional SL model. One of the reasons for the good performance of SSL model in this study is that not only the training data of SL, but also the labeled data of SSL reflected all patterns within the population appropriately. It shows the possibility that the SSL would require less time, effort, and cost during the data preprocessing and also provide a satisfactory outcome as SL when a small amount of labeled dataset of SSL reflects all patterns in the population well. More studies are needed for SSL to be used clinically in the dental images in the future.

More clinical and transdisciplinary medical and advanced technological studies are needed to improve accurate predictions and consistent performance of AI and minimize the effort during preprocessing step. In the future, it would assist humans in the medical and dental fields for better performance.

Competing interests

The authors declare no conflict of interest.

Funding

This study was funded by a 2021 research grant from the Research institute of medical science, The Catholic University of Korea Eunpyeong St Mary's Hospital (EMBRF-2021-09). The funder only provided support in research materials to Lee SH but did not have any additional role in the study design, data collection and analysis, decision to publish, or preparation of the manuscript.

Ethical approval

This study was approved by the Institutional Review Board (IRB) and Clinical Data Warehouse (CDW) data review board of the Catholic University of Korea, Catholic Medical Center (CIRB-20210503–001). The authors are on consent to participate and consent to publish. The IRB waived the written documentation of informed consent.

REFERENCES

1. Kim JY, Jee HG, Song HC, Kim SJ, Kim MR. Clinical and pathologic features related to the impacted third molars in patients of different ages: A retrospective study in the Korean population. *J Dent Sci* 2017; **12**: 354–59. https://doi.org/10.1016/j.jds.2017.01.004
2. El-Khateeb SM, Arnout EA, Hifnawy T. Radiographic assessment of impacted teeth and associated Pathosis prevalence. pattern of occurrence at different ages in Saudi male in Western Saudi Arabia. *Saudi Med J* 2015; **36**: 973–79. https://doi.org/10.15537/smj.2015.8.12204
3. Liu T, Siegel E, Shen D. Deep learning and medical image analysis for COVID-19 diagnosis and prediction. *Annu Rev Biomed Eng* 2022; **24**: 179–201. https://doi.org/10.1146/annurev-bioeng-110220-012203
4. Malhotra P, Gupta S, Koundal D, Zaguia A, Enbeyle W. Deep neural networks for medical image Segmentation. *J Healthc Eng* 2022; **2022**: 9580991. https://doi.org/10.1155/2022/9580991
5. Yamashita R, Nishio M, Do RKG, Togashi K. Convolutional neural networks: An overview and application in Radiology. *Insights Imaging* 2018; **9**: 611–29. https://doi.org/10.1007/s13244-018-0639-9
6. Ahmed N, Abbasi MS, Zuberi F, Qamar W, Halim MSB, Maqsood A, et al. Artificial intelligence techniques: Analysis, application, and outcome in dentistry-A systematic review. *BioMed Research International* 2021; **2021**: 1–15. https://doi.org/10.1155/2021/9751564
7. Fukuda M, Ariji Y, Kise Y, Nozawa M, Kuwada C, Funakoshi T, et al. Comparison of 3 deep learning neural networks for classifying the relationship between the Mandibular third molar and the Mandibular Canal on panoramic Radiographs. *Oral Surgery, Oral Medicine, Oral Pathology and Oral Radiology* 2020; **130**: 336–43. https://doi.org/10.1016/j.oooo.2020.04.005
8. Vinayahalingam S, Xi T, Bergé S, Maal T Jong G. Automated detection of third molars and mandibular nerve by deep learning. Sci Rep. 2019;9:9007.
9. Yoo J-H, Yeom H-G, Shin W, Yun JP, Lee JH, Jeong SH, et al. Deep learning based prediction of extraction difficulty for

Mandibular third molars. *Sci Rep* 2021; **11**: 1954. https://doi.org/10.1038/s41598-021-81449-4
10. Sellars P, Aviles-Rivero AI, Schonlieb CB. LaplaceNet: A Hybrid Graph-Energy Neural Network for Deep Semisupervised Classification. IEEE Trans Neural Netw Learn Syst. 2022:1-13.
11. Kim YJ, Kim KG. Development of an Optimized deep learning model for medical imaging. *Taehan Yongsang Uihakhoe Chi* 2020; **81**: 1274–89. https://doi.org/10.3348/jksr.2020.0171
12. Assran M, Caron M, Misra I, Bojanowski P, Joulin A, Ballas N, et al. Semi-Supervised Learning of Visual Features by Non-Parametrically Predicting View Assignments with Support Samples. In: Paper presented at the In: Paper presented at the 2021 IEEE/CVF International Conference on Computer Vision (ICCV), Montreal, QC, Canada. https://doi.org/10.1109/ICCV48922.2021.00833
13. Han CH, Kim M, Kwak JT, Ortega-Martorell S. Semi-supervised learning for an improved diagnosis of COVID-19 in CT images. *PLoS ONE* 2021; **16**: e0249450. https://doi.org/10.1371/journal.pone.0249450
14. Huynh T, Nibali A, He Z. Semi-supervised learning for medical image classification using imbalanced training data. *Computer Methods and Programs in Biomedicine* 2022; **216**: 106628. https://doi.org/10.1016/j.cmpb.2022.106628
15. Kuo C-FJ, Liao Y-S, Barman J, Liu S-C. Semi-supervised deep learning semantic Segmentation for 3D volumetric computed Tomographic scoring of chronic Rhinosinusitis: Clinical correlations and comparison with Lund-Mackay scoring. *Tomography* 2022; **8**: 718–29. https://doi.org/10.3390/tomography8020059
16. Choi E, Lee S, Jeong E, Shin S, Park H, Youm S, et al. Artificial intelligence in positioning between Mandibular third molar and inferior alveolar nerve on panoramic radiography. *Sci Rep* 2022; **12**: 2456. https://doi.org/10.1038/s41598-022-06483-2
17. Zagoruyko S, Komodakis N. Wide residual networks
18. Kotyan S, Vargas DV. Adversarial robustness assessment: Why in evaluation both L0 and L∞ attacks are necessary. *PLoS One* 2022; **17**(4): e0265723. https://doi.org/10.1371/journal.pone.0265723
19. Jangam E, Barreto AAD, Annavarapu CSR. Automatic detection of COVID-19 from chest CT Scan and chest X-rays images using deep learning, transfer learning and stacking. *Appl Intell* 2022; **52**: 2243–59. https://doi.org/10.1007/s10489-021-02393-4
20. Zhong Z, Wei F, Lin Z, Zhang C. ADA-Tucker: Compressing deep neural networks via adaptive dimension adjustment tucker decomposition. Neural Netw. 2019;110:104-115.
21. Qayyum A, Tahir A, Butt MA, Luke A, Abbas HT, Qadir J, et al. Dental Caries detection using a semi-supervised learning approach. *Sci Rep* 2023; **13**: 749. https://doi.org/10.1038/s41598-023-27808-9
22. Bleeker SE, Moll HA, Steyerberg EW, Donders ART, Derksen-Lubsen G, Grobbee DE, et al. External validation is necessary in prediction research: A clinical example. *J Clin Epidemiol* 2003; **56**: 826–32. https://doi.org/10.1016/s0895-4356(03)00207-5
23. Schwendicke F, Samek W, Krois J. Artificial intelligence in dentistry: Chances and challenges. *J Dent Res* 2020; **99**: 769–74. https://doi.org/10.1177/0022034520915714